IAES International Journal of Artificial Intelligence (IJ-AI)
Vol. 15, No. 6, December 2026, pp. 5534~5547
ISSN: 2252-8938, DOI: 10.11591/ijai.v15.i6.pp5534-5547

Improving air quality assessment using visual features extraction

Khadija Marzagui[1], Yassine Benhlal[1], Abdelkaher Ait Abdelouahad[1], Abdellatif Dahmouni[2], Ahmed Drissi El Maliani[3], Hammadi Nait-Charif[4]
[1]LAROSERI, Department of Computer Science, Faculty of Sciences, University of Chouaib Doukkali, El Jadida, Morocco
[2]IMACS, School of Technology, Moulay Ismail University, Meknes, Morocco
[3]LRIT, Faculty of Sciences, Mohammed V University, Rabat, Morocco
[4]National Centre for Computer Animation, Bournemouth University, Poole, United Kingdom

Article Info

Article history:

Received Oct 6, 2025
Revised Sep 8, 2026
Accepted Sep 20, 2026

Keywords:

Air quality
Feature extraction
Grid search
Image based AQI classification
Image quality assessment
Machine learning

ABSTRACT

Air pollution is an important environmental issue with serious consequences for human health and quality of life, particularly in large urban areas, where it leads to numerous respiratory and cardiovascular diseases. Reliable air quality monitoring methods are therefore essential to accurately assess pollution levels, understand their health impacts, and support effective public health decision-making. This propose a new image-based method to estimate levels of air quality index (AQI) based on image quality and atmospheric visual degradation. The approach is based on complementary visual quality features (like blind/referenceless image spatial quality evaluator (BRISQUE), contrast enhancement-based image quality (CEIQ), naturalness image quality evaluator (NIQE), and no-reference image quality metric for contrast distortion (NIQMC)) in combination with meteorological/statistical parameters (like entropy, root mean square (RMS) contrast, and mean transmission). Furthermore, the picture-based prediction of $PM_{2.5}$ concentration descriptor is proposed for estimating particulate matter directly, and all extracted features are fused and classified using machine learning models optimized via grid search–based hyperparameter tuning to improve classification performance. The proposed method is evaluated through two publicly datasets Dhaka and India-Nepal with accuracies of 88.82% and 95.40%, respectively, proving the efficiency for performance and reliability of proposed approach.

This is an open access article under the CC BY-SA license.

Corresponding Author:

Khadija Marzagui
LAROSERI, Department of Computer Science, Faculty of Sciences, University of Chouaib Doukkali
El Jadida, Morocco
Email: marzagui.khadija@ucd.ac.ma

1. INTRODUCTION

Air pollution is among the most serious and urgent environmental concerns in the world. It primarily originates from human activities, including industrial emissions, vehicle exhaust, and the burning of fossil fuels in power plants. These activities release pollutant particles that are inhaled into the respiratory tract and lungs. Long-term exposure to these pollutants can lead to severe health problems, including respiratory diseases, cardiovascular diseases, and even cancer. The direct effects of air pollution on human health have made it a global focus of environmental management activities.

Air quality degradation is accelerated by climate change in addition to anthropogenic sources. Rising global temperatures promote the production of tropospheric ozone, a toxic atmospheric pollutant. Moreover, the growing prevalence and severity of forest fires injects massive doses of fine travel particulates into the air, further sulfur quality. As examples, extended droughts and stagnant air masses as a result of some

weather events restrict the dispersal of pollutants resulting in increased concentrations in particular areas. These reasons highlight the need to create improved solutions to track and control air contamination [1].

It is important to measure air quality in different areas, so we can more clearly see this problem and deal with it. This assessment not only raises public awareness, but also helps to shape the air quality-related policies that might help reduce emissions of pollutants. Air quality index (AQI) is traditionally calculated based on selected pollutants from monitoring stations that use specially designed sensors to continuously monitor the concentrations of specific atmospheric pollutant levels [2]. These measurements are ultimately used to construct an AQI, a standard metric of the air quality which segments the air quality into different categories related to health risk.

The AQI is a numerical system that was proposed by the U.S. Environmental Protection Agency (EPA) to characterize air quality based on five pollutants: carbon monoxide (CO), nitrogen dioxide (NO_2), ozone (O_3), particulate matter ($PM_{2.5}$ and PM_{10}), and sulfur dioxide (SO_2). For each of the five pollutants, a sub-index is calculated based on their concentrations and corresponding thresholds established by the National Ambient Air Quality Standards (NAAQS), using epidemiological studies that establish health effects from pollutant exposure as a basis for establishing those thresholds. The AQI as a whole is determined by the highest sub-index, which indicates the highest pollutant at that moment [3].

While air quality monitoring stations can successfully monitor air quality, they have many shortcomings. First there aren't enough stations to monitor large areas and most of them are located in urban settings or large industrial areas, hence many places in the country are left unmapped. Furthermore, these stations do not allow large scale, and real time monitoring of air quality for risk mitigation, which is critical for proactive risk management. Moreover, the cost to install and maintain these stations is also prohibitive for widespread scalable implementations.

To address these limitations, several researchers attempted to use meteorological emission models to simulate emitted pollutants [4]. One example is the community multi-scale air quality (CMAQ) model which was developed to predict the formation of $PM_{2.5}$ and to evaluate its response to the reduction in precursor emissions and later used in the understanding of the effects from emissions control strategies and regulatory applications [5]. Additionally, the weather research and forecasting (WRF)-Chem model was also developed as a fully coupled online system to facilitate the simultaneous air quality and meteorological modeling to enhance its utility for operational forecasting [6]. However, because of the lack of accurate pollutant emissions data and theoretical basis, the simulation approaches have achieved limited results and low estimation accuracy.

In response to these challenges, researchers have employed a data-driven strategy and statistical approaches. Artificial neural networks (ANN), multiple linear regression, and support vector regression (SVR) are frequently used statistical methods for forecasting air quality [7], [8]. In light of the high degree of spatial correlations observed between air quality monitoring sites, spatiotemporal predictive models (including spatiotemporal ANN, spatiotemporal SVR) have gained attention among researchers [9].

In recent years, research has increasingly emphasized air quality estimation with spatiotemporal heterogeneous urban big data, which would include datasets with spatial, temporal and categorical data [10]–[12]. The premise is that air quality is heavily influenced by urban dynamics such as its wind patterns, traffic patterns, and points of interest (POI). Therefore, air quality can be estimated at places that do not have monitoring stations by analyzing the temporal and spatial dependencies of the urban data (e.g., meteorology and traffic patterns). However, these distinct methodologies require high computational power and lengthy time periods to analyze large scale and complex data. Plus, obtaining large amount of sensing data, need to be accounted for.

With the rapid advancements in computer vision, the use of outdoor cameras for air quality assessment has significantly increased. These devices take high resolution images, presenting a new way to view air quality. Real-time images captured by outdoor cameras can be analyzed to detect and quantify several indicators of pollution, including fine particles or gaseous pollutants. By leveraging advanced video and image analysis algorithms along with deep learning approaches, it is feasible to process these images in order to estimate pollutant concentrations in regions not reachable by conventional monitoring stations. This approach overcomes some limitations of meteorological and statistical models by providing a more direct and localized method for air quality assessment. Moreover, integrating the visual quality of the image enables the development of automated systems capable of continuously and autonomously monitoring of air quality, offering a solution for effective pollution management. In this context, the research proposes a novel method that combines visual quality features, meteorological features and air quality related features from images to estimate the AQI using machine learning models.

The rest of this paper is structured as follows. Section 2 presents an overview of existing methods and approaches related to image-based air quality estimation. Section 3 presents the datasets used in this work. Section 4 outlines the details of our proposed method, based on image quality assessment for AQI

estimation. In section 5, compare the method with the state-of-the-art methods. Finally, section 6 provides the conclusion of the study and perspectives for future work.

2. RELATED WORK

Currently, existing methods for measuring air quality based on images are divided into three main categories: traditional image processing methods, deep learning-based methods and those leveraging the visual quality of images. Traditional approaches rely on handcrafted features, such as color, texture and haze-related descriptors, combined with conventional regression or classification models. Deep learning-based methods automatically learn discriminative representations from raw images using convolutional neural networks (CNN), generally at the cost of large training datasets and high computational resources. Visual quality-based approaches exploit no-reference image quality assessment metrics to quantify the degradation caused by atmospheric pollution on the captured images. The following subsections review the main works within each category.

2.1. Traditional approaches

One of the earliest studies in image-based air pollution estimation relied on handcrafted features like color, texture and haze related indices. A novel descriptor called the dark channel prior (DCP) was utilized to model haze intensity. Li *et al.* [13] introduced a combination of transmission matrix and depth information to predict haze levels, Liu *et al.* [14] incorporated DCP, SVR, and meteorological data for $PM_{2.5}$ prediction. Zhang *et al.* [15] proposed a multi-kernel learning scheme that combines DCP and contrast features, Chen *et al.* [16] used neural networks with HSV color transformations to reduce $PM_{2.5}$ estimation. These models demonstrate that handcrafted and multimodal descriptors still generalize well to describe atmospheric conditions from images.

2.2. Deep learning approaches

With the arrival of deep learning, CNNs are widely applied for the automatic extraction of spatial features from images. Zhang *et al.* [17] proposed photo air pollution level estimation algorithm (PAPLE) which is a CNN combined with an ordinal classifier and modified rectified linear unit (ReLU) activation function, while Chakma *et al.* [18] used CNN-derived features with transfer learning and random forest classifiers for the classification of $PM_{2.5}$. For real-time estimate, Ma *et al.* [19] correlates CNN representations with SVR. Ahmed *et al.* [20] developed AQE-Net based on ResNet18 that combines spatial and contextual attention. These studies have indicated that deep learning techniques are capable of furnishing accurate and scalable air pollution prediction from different sources of imagery data.

2.3. Visual quality-based approaches

In addition to traditional and deep learning pipelines, many authors have focused on no-reference image quality assessment (NR-IQA) metrics related to the degradation of an image to pollution levels. Xia [21] used linear/nonlinear models and SVR to track $PM_{2.5}$. Gu *et al.* [22] introduced picture-based prediction of $PM_{2.5}$ concentration (PPPC), an entropy-based predictor associating disturbance from natural scene statistics (NSS) with $PM_{2.5}$ concentrations. Nilesh *et al.* [23] utilized blind/referenceless image spatial quality evaluator (BRISQUE) in addition to YOLOv5 to detect polluting vehicles and estimate AQI from traffic imagery. Sun *et al.* [24] further combined means of color distortion, structure degradation and NSS features into a prediction model for $PM_{2.5}$ estimation. Experimental results show that quality visual-aided methods obtain competitive and even outperform traditional and deep learning techniques.

3. DATASET

This paper use two publicly available datasets namely Dhaka dataset from Bangladesh and India-Nepal dataset. These datasets provide accurate information on AQI concentrations with related images. They were selected because they differ in size, image acquisition conditions and geographic context, which allows the proposed method to be evaluated under diverse scenarios. Both datasets associate each image with a ground-truth air quality label derived from official measurements, organized into six pollution categories.

3.1. Dhaka dataset

The Dhaka dataset [25] from Bangladesh spans the period 2020 to 2022 and contains 1,818 images that were taken by local residents or by the research team using smartphones. The photographs are variable in resolution, but over their expanse represent a large portion of the sky around the time of observation to allow for visual randomization with respect to atmospheric conditions. A $PM_{2.5}$ measurement from American

consulate Dhaka is associated with each image [26] and six classes of $PM_{2.5}$ to gauge air quality on an official scale. This dataset contains a variety of urban scenes and covers a wide range of pollution levels, thereby representing the dynamic nature of the environment over time.

3.2. Eff-AQI dataset

The second dataset, named air pollution image dataset from India and Nepal is available in public on Kaggle [27]. It is composed of 12,240 images which were collected from various geographic locations in India (Delhi, Nagaland, Bengaluru, Greater Noida, Faridabad, Mumbai, and Tamil Nadu) and Biratnagar (Nepal). All images were captured in daylight conditions to reduce lighting variability and standardized to resolution 224 × 224 pixels. Each image is annotated with a corresponding air quality category from the central pollution control board (CPCB) [28], with categories of good, moderate, unhealthy for sensitive groups, unhealthy, very unhealthy, and severe.

4. PROPOSED MODEL

This paper presents a new approach to estimating AQI level from an image. As shown in Figure 1, the proposed pipeline begins with image acquisition and preprocessing stage where input images are resized to a common scale and pixel intensities are normalized. From the prepared images, a range of features are obtained including meteorological-based measures (root mean square (RMS) contrast, entropy, and mean transmission), visual quality indicators scores (BRISQUE, contrast enhancement-based image quality (CEIQ), naturalness image quality evaluator (NIQE), and no-reference image quality metric for contrast distortion (NIQMC)) as well as so-called PPPC a descriptor explicitly built to estimate $PM_{2.5}$ related information. For every image, these feature representations are then concatenated into a single 8-dimensional feature vector, and all samples are used to build a corresponding feature matrix of dimension m × 8 along with AQI levels (e.g., good, moderate, unhealthy). Several machine learning classifiers (support vector classifier (SVC), random forest, gradient boosting, and voting classifier) are trained using the resultant dataset. A grid search strategy is used to optimize the classifiers' hyperparameters in order to establish the optimal parameter configuration.

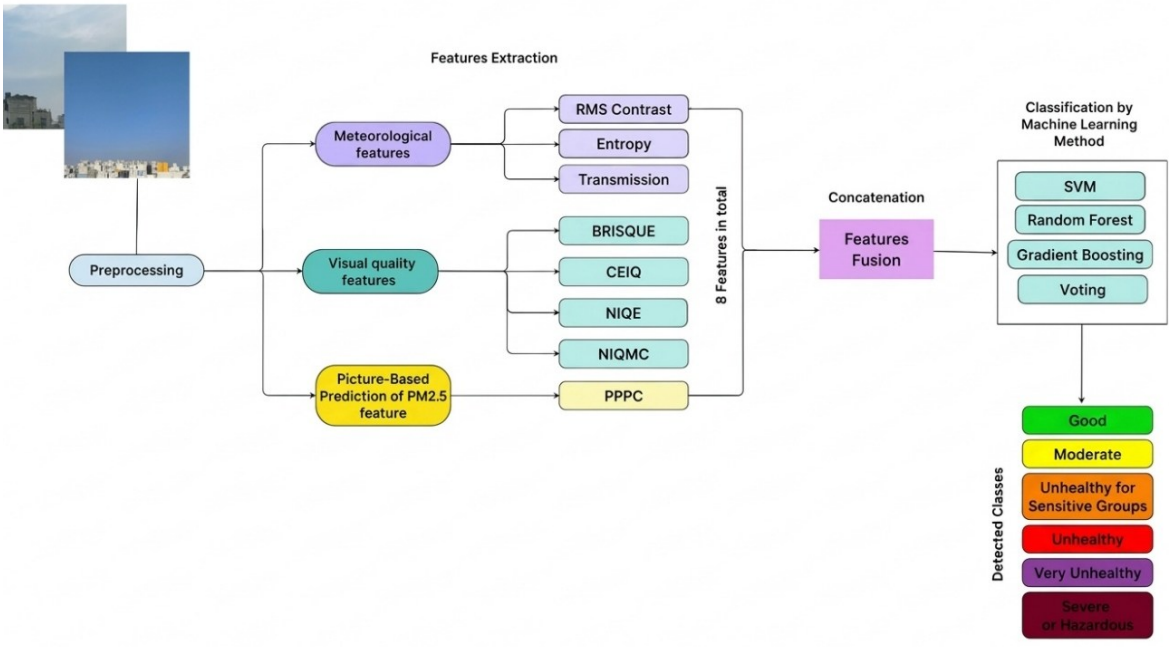

Figure 1. The proposed method pipeline

4.1. Preprocessing

The input images are resized to a uniform size to ensure consistency in the analysis. Pixel intensity normalization is performed to minimize variations in lighting and contrast. Although noise, representing the

pollution index, is present in the images, it is retained as it is an important feature for air quality assessment. Thus, the preprocessing steps prepare the images while preserving the crucial pollution-related information.

4.2. Class imbalance bias with synthetic minority over-sampling technique

As some categories are underrepresented in the datasets, the synthetic minority over-sampling technique (SMOTE) method was applied [29]. This technique generates synthetic examples for the minority classes, balancing the class distribution and reducing the bias caused by class imbalance. Table 1 summarizes the class distribution before and after applying SMOTE for the Dhaka and India-Nepal datasets.

Table 1. Class distribution of the whole Dhaka and Eff-AQI datasets before and after applying SMOTE

Classe	Unbalanced		Balanced	
	Eff-AQI	Dhaka	Eff-AQI	Dhaka
Good	1541	17	2863	741
Moderate	1573	490	2863	741
Unhealthy for sensitive group	2863	317	2863	741
Unhealthy	2622	741	2863	741
Very unhealthy	2194	225	2863	741
Severe or hazardous	1447	21	2863	741

Note: in the experiments, SMOTE was applied only to the training set after the train/test split

4.3. Feature extraction step

After preprocessing, features are extracted from the images. These features are regrouped into three main categories namely, meteorological features, visual quality features and picture-based prediction of $PM_{2.5}$ feature. It is expected that each category will contribute specific information for air quality assessment, combining visual and environmental data for a comprehensive analysis.

4.3.1. Meteorological features extraction

These features assess the clarity and transparency of the air in the image, which can be influenced by the presence of fine particles ($PM_{2.5}$, PM_{10}). They include the following measures:

i) RMS contrast: the RMS contrast quantifies the intensity of contrast variations in an image, allowing for the measurement of the overall clarity of the scene. Mathematically, it is defined as the standard deviation of pixel intensities in an image and is expressed by (1) [30].

$$RMS = \sqrt{\frac{1}{M \times N} \sum_{i=1}^{M} \sum_{j=1}^{N} \left(I_{ij} - avg(I)\right)^2} \quad (1)$$

Where I_{ij} is the intensity at pixel (i, j), M is the number of rows, N is the number of columns, and $avg(I)$ represents the average intensity of all pixels in the image. This definition shows that the RMS contrast does not depend on spatial frequency content or contrast distribution within the image.

ii) Entropy: entropy measures the diversity of grayscale levels in an image, helping to assess the amount of visual information. It is mathematically defined by (2) [31].

$$Entropy = -\sum_{i=1}^{M} p_i \, log_2(p_i) \quad (2)$$

Where p_i represents the probability that the pixel intensity equals i. When the concentration of certain features, such as suspended particles, increases, the image details may decrease, leading to a reduction in entropy.

iii) Transmission-mean: transmission-mean indicates the average transparency of the air in the image and helps estimate the density of fog or pollution. The calculation relies on two essential components of image dehazing: the dark channel and atmospheric transmission [32].

iv) Dark channel calculation*:* the dark channel identifies darkest areas in each color channel (R, G, or B) within a given region around each pixel, allowing the detection of areas most affected by fog. It is defined by (3).

$$D(x) = \min_{c \in \{R,G,B\}} \left(\min_{y \in \Omega(x)} I^c(y) \right) \quad (3)$$

Where $\Omega(x)$is a region of pixels around the pixel x.

v) Atmospheric transmission estimation: the transmission is estimated for each pixel to calculate the fraction of light reaching the camera after passing through the fog. It is defined by (4).

$$t(x) = 1 - \omega \cdot \frac{D(x)}{255} \quad (4)$$

With ω as the opacity parameter, here set to 0.95. Finally, the average of these transmission values is calculated to obtain the overall transmission of the image.

4.3.2. Visual quality features extraction

These indices measure aspects of visual quality that could be affected by the presence of airborne particles, such as noise, blur and visual artifacts. This study use the following indices: i) BRISQUE: is a method that uses natural image statistics to analyze visual impairments such as noise and blur, without requiring a reference image for evaluation. This approach relies on the analysis of statistical characteristics of the image to assess its quality [33]; ii) CEIQ: rates the quality of images based on contrast enhancement and changes. It can be useful in identifying visual disturbances that may influence the overall assessment of an image, particularly in areas with changed contrast [34]; iii) NIQE: employs natural-image-based statistics to assess the quality of degraded images when the types of distortion are not known. NIQE relies on natural statistical characteristics of the image to evaluate quality [35]; and iv) NIQMC: this image quality metric quantifies the quantity of visual quality of an image, factoring in contrast distortion. NIQMC utilizes contrast in the local and global image to provide a visual quality metric without the use of a reference image [36].

4.3.3. Image-based prediction of $PM_{2.5}$ feature

This feature is specifically developed to estimate $PM_{2.5}$ concentration in real-time from images. PPPC uses visual information to estimate pollution levels by capturing variations that may correspond to $PM_{2.5}$ concentrations. This index is particularly relevant for images captured by mobile devices and is aimed at providing an immediate estimate of air quality [22].

4.4. Machine learning models and hyperparameter optimization

Before training the machine learning classifiers, namely the SVC, random forest, gradient boosting, and voting classifier, an explicit hyperparameter optimization step was introduced. This step was considered essential due to the sensitivity of these models to hyperparameter selection. Therefore, grid search was employed to systematically determine the optimal parameter configurations prior to final model training.

4.4.1. Hyperparameter optimization using grid search

This study performed hyperparameter tuning using an exhaustive Grid Search strategy across pre-defined parameter ranges. This study have chosen the best set of parameters based on the weighted F1-score obtained on the training set to ensure balanced classification across all AQI categories. The final predictive models were then trained using the best parameter configuration.

4.4.2. Machine learning models

In order to evaluate the classification performance of the proposed AQI estimation framework, four supervised machine learning models were shortlisted. These models were selected for their different ways of learning from data, and have been proven effective in image-based and environmental classification tasks. The other model chosen was SVC, known for its strong generalization in high dimensionality feature spaces and its ability to handle nonlinear decision boundaries based on corresponding kernel functions [37]. The random forest classifier was chosen because of its ensemble learning principles built on multiple decision trees that provide improved robustness to noise and lower overfitting through a consensus from multiple learner predictions [38]. This study included the gradient boosting model which learns complex feature interactions through a sequential ensemble approach where each weak learner attempts to correct the errors of its predecessors resulting in improved predictive performance [39]. To finally combine individual model strengths, a voting classifier was utilized. The voting strategy combines the SVC, random forest, and gradient boosting predictions to improve classification stability and overall performance between different AQI categories [40].

5. EXPERIMENTAL RESULTS AND DISCUSSION

The process of experimentation entailed importing the dataset, removing missing values, and selecting relevant image quality and atmospheric features, including BRISQUE, CEIQ, NIQE, RMS contrast, entropy, NIQMC, PPPC, and transmission mean, for AQI classification. The categorical AQI labels were

encoded into numerical classes. The data were then divided into training (67%) and testing (33%). Feature standardization was performed using StandardScaler to control variable scaling by using one uniform method. To address class imbalance, SMOTE was applied only to the training set. Hyperparameter tuning was conducted using a grid search strategy, and the final models were trained using the optimal parameter configurations before evaluation on the independent test set.

The experimental results were obtained using both the Dhaka and India-Nepal datasets to assess the performance of the proposed model. In order to accurately detect pollution levels, a decent AQI classification model must perform well in terms of accuracy and F1-score. RMS contrast, entropy, transmission mean, BRISQUE, CEIQ, NIQE, NIQMC, and PPPC were among the visual features used in this study to evaluate their respective contributions to AQI classification. In order to assess their effectiveness, the integration of all these features was also examined.

5.1. Results of Dhaka dataset

5.1.1. Results of individual feature contributions to air quality index classification

The first step was to assess the discriminative power of individual features. Some features such as BRISQUE produced relatively better results (reaching a maximum of 49.45% accuracy and F1-score of 0.48 with the random forest classifier), as shown in Table 2. Other features, on the other hand, despite their novelty and state-of-the-art nature (PPPC) gave much more limited performance with an accuracy of 39.91% (F1 = 0.39). These observations suggest single feature alone is not enough to result in high AQI classification performance.

Table 2. Performance of models using individual features on the Dhaka dataset

Model	RMS contrast		Entropy		Transmission-mean		BRISQUE		CEIQ		NIQE		NIQMC		PPPC	
	Acc	F1	Acc	F1	Acc	F1	Acc	F1	Acc	F1	Acc	F1	Acc	F1	Acc	F1
SVC	35.49	0.31	39.23	0.33	38.96	0.36	43.46	0.37	38.55	0.33	40.12	0.31	38.14	0.34	24.79	0.18
Random forest	43.11	0.42	46.11	0.45	43.32	0.43	49.45	0.48	41.55	0.41	44.34	0.42	42.84	0.42	39.91	0.39
Gradient boosting	36.64	0.36	39.37	0.39	35.49	0.35	42.92	0.42	34.40	0.34	36.98	0.36	35.28	0.35	33.51	0.33
Voting	37.60	0.37	40.73	0.41	36.71	0.36	44.41	0.44	36.03	0.36	39.85	0.38	37.19	0.37	33.65	0.33

Note: acc: accuracy; F1: F1-score

5.1.2. Results of fused all-feature contributions to air quality index classification

The results of fused features on the Dhaka dataset show an enhanced classification score. According to Table 3, the gradient boosting model achieved the best overall performance accounting for an accuracy of 86.31% and F1-score of 0.86 values higher than other evaluated models. Results for the voting classifier were in close proximity with accuracy=85.29% and F1-score=0.85, followed by random forest (83.58%,0.84) and SVC (83.24%,0.83), being relatively less but still considerable results.

Table 3. Performance of models using all features on the Dhaka dataset

Model	Accuracy (%)	Precision	Recall	F1-score
SVC	83.24	0.83	0.83	0.83
Random forest	83.58	0.84	0.84	0.84
Gradient boosting	86.31	0.86	0.86	0.86
Voting	85.29	0.85	0.85	0.85

5.1.3. Performance results of hyperparameter-optimized classification models using grid search

The performance results obtained after performing hyperparameter optimization based on grid search show an apparent improvement in AQI classification by utilizing all fused quality features of images. Out of all optimized models, high and balanced performance is reached for accuracy, precision, recall, and F1-score metrics. More specifically, gradient boosting on overperform with 88.82%, which is followed by voting classifier and random forest classifier that have an accuracy of 88.62% and 88.48%, respectively, while SVM achieved a competitive accuracy of 87.19%. Stable and reliable classification performance is also confirmed by impartial precision, recall, and F1-score values (~0.87–0.89). In summary, the results depicted in Table 4 verify that grid search-based hyper-parameter optimization using all output fused

features improved classification performance and establishes a potential high-performance framework for AQI estimation.

The confusion matrix of the Dhaka dataset is shown in Figure 2, which provides the classification performance gained by all fused features with grid search based optimization. Figure 2(a) shows SVC. Figure 2(b) presents gradient boosting. Figure 2(c) illustrates random forest. Figure 2(d) depicts the voting classifier. The classifiers are optimized and have strong diagonal dominance, showing that the models were tuned nicely with decreased misclassifications. The class-wise predictions are more balanced, especially for intermediate AQI levels for gradient boosting and the voting classifier with the remaining misclassifications mainly being restricted to adjoining classes.

Table 4. Classification results using all fused features with grid search optimization on the Dhaka dataset

Model	Accuracy (%)	Precision	Recall	F1-score
SVC	87.19	0.87	0.87	0.87
Random forest	88.48	0.89	0.88	0.88
Gradient boosting	88.82	0.89	0.89	0.89
Voting	88.62	0.89	0.89	0.89

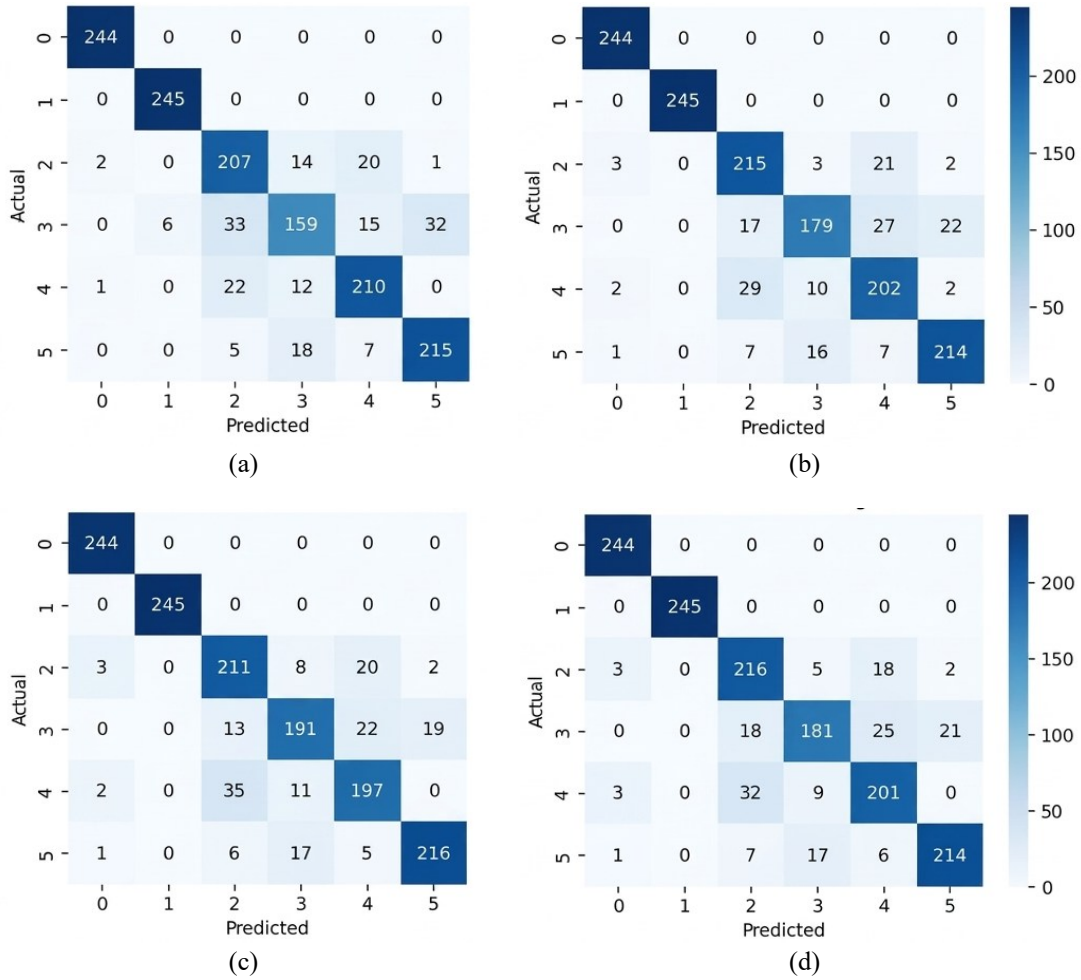

Figure 2. The confusion matrices applied to classify AQI levels using the Dhaka dataset for four classifiers: (a) SVC, (b) gradient boosting, (c) random forest, and (d) voting

5.2. Results of India-Nepal dataset

5.2.1. Results of individual feature contributions to AQI classification

The individual features were analyzed first to determine the discriminative power of each feature alone. The results obtained using single descriptors, which are reported in Table 5, tend to be quite low. NIQMC, e.g., gets an accuracy of 36.62%, F1-score of 0.35 with random forest classifier while BRISQUE

reaches 27.32% accuracy with the same model. Some features show better performance than others but still significantly lower than the results through integrating features.

Table 5. Performance of models using individual features on the India-Nepal dataset

Model	RMS contrast		Entropy		Transmission-mean		BRISQUE		CEIQ		NIQE		NIQMC		PPPC	
	Acc	F1	Acc	F1	Acc	F1	Acc	F1	Acc	F1	Acc	F1	Acc	F1	Acc	F1
SVC	32.96	0.31	29.29	0.25	31.08	0.30	22.17	0.19	29.75	0.28	27.88	0.27	34.29	0.33	27.51	0.19
Random forest	37.73	0.37	34.08	0.33	34.97	0.34	27.32	0.27	33.60	0.33	30.11	0.29	36.62	0.35	32.77	0.31
Gradient boosting	35.06	0.34	31.82	0.31	32.47	0.32	28.61	0.28	31.02	0.31	28.24	0.28	33.92	0.33	30.88	0.31
Voting	37.34	0.37	33.79	0.33	34.73	0.34	29.14	0.29	33.25	0.33	29.93	0.29	36.19	0.35	32.01	0.31

Note: acc: accuracy; F1: F1-score

5.2.2. Results of fused all-feature contributions to AQI classification

Fused features evaluation on the India-Nepal dataset strengthens the evident superiority of individual feature contributions to AQI classification. Table 6 shows that we achieve amazing performances using the gradient boosting model, with an accuracy of 94.18% and a F1-score of 0.94, which indicates its excellent formulation to handle complex relationships due to non-linearities by means of iterative error correction. The voting classifier was ranked second (91.90%, 0.92), followed by random forest (88.18%, 0.88) and SVC (88.80%, 0.89), which showed relatively poorer results but still with satisfactory performance in terms of accuracy and F1-score respectively.

Table 6. Performance of models using all features on the India-Nepal

Model	Accuracy (%)	Precision	Recall	F1-score
SVC	88.80	0.89	0.89	0.89
Random forest	88.18	0.88	0.88	0.88
Gradient boosting	94.18	0.94	0.94	0.94
Voting	91.90	0.92	0.92	0.92

5.2.3. Performance results of hyperparameter-optimized classification models using grid search

After tuning hyperparameters using grid search on the India-Nepal dataset, this study see high and consistent classification performance across all models used. Table 7 demonstrates that using all fused features in combination with a grid search optimization of the classification models is better performing than both the individual feature methods and just using fused features without an optimization. In particular, gradient boosting has the highest accuracy (95.40%), followed by SVM (95.36%) and the voting classifier (95.29%) closely, while random forest shows a lower accuracy level (94.28%). These results support the fact that through using grid search to optimize classification models they more efficiently exploit feature space provided by fusion and generalize well across geographical areas.

Table 7. Classification results using all fused features with grid search optimization on India-Nepal dataset

Model	Accuracy (%)	Precision	Recall	F1-score
SVC	95.36	0.95	0.95	0.95
Random forest	94.28	0. 94	0.94	0.94
Gradient boosting	95.40	0.95	0.95	0.95
Voting	95.29	0. 95	0.95	0.95

Confusion matrix representing the classification performance with all fused features (grid search based optimization) on India-Nepal dataset is shown in Figure 3. Figure 3(a) shows SVC. Figure 3(b) presents random forest. Figure 3(c) illustrates gradient boosting. Figure 3(d) depicts the voting classifier. Optimized classifiers exhibit good diagonal dominance indicating good hyperparametric tuning and clear decision boundaries. The class-wise predictions of gradient boosting and the voting classifier are fairly balanced, particularly considering the intermediate AQI levels, though pairwise misclassifications usually occur for visually similar classes.

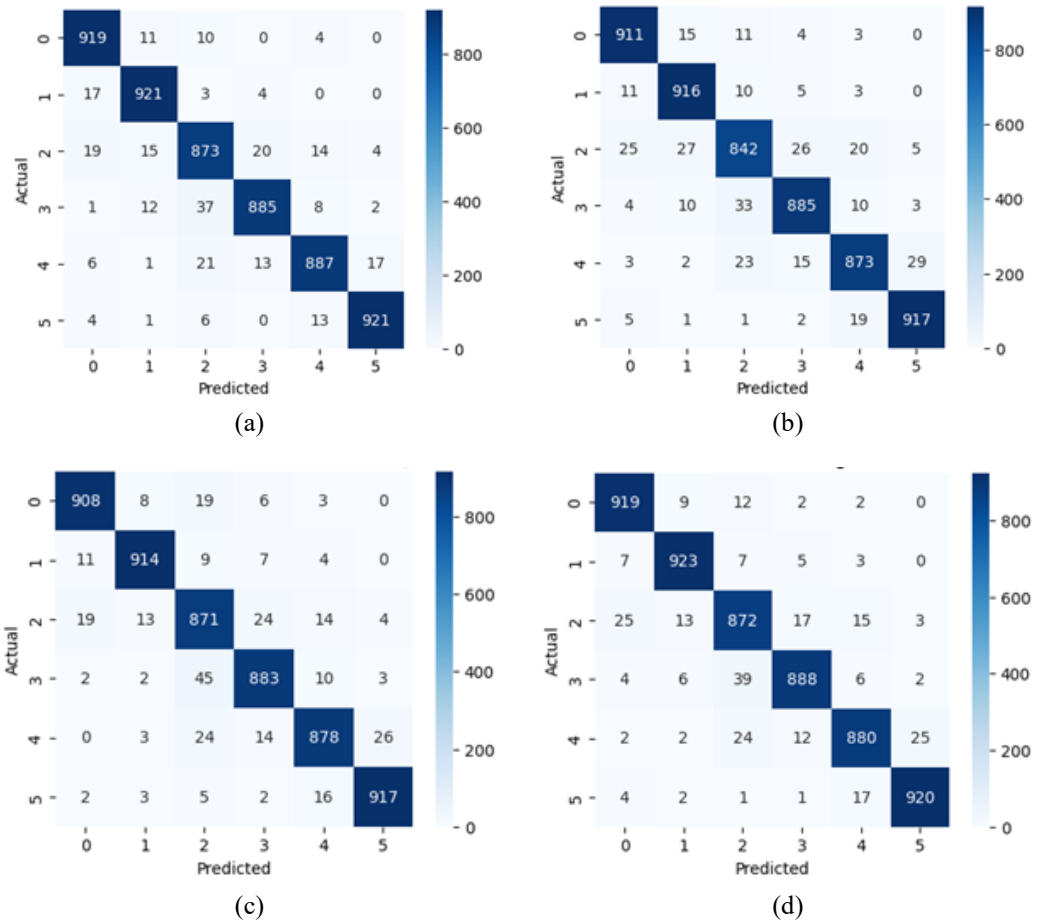

Figure 3. The confusion matrices applied to classify AQI levels using the India-Nepal dataset for four classifiers: (a) SVC, (b) random forest, (c) gradient boosting, and (d) voting

5.3. Statistical significance analysis

McNemar's test was used to compare the performance of the gradient boosting classifier versus competing models, support vector machine, random forest and voting classifier using paired predictions on independent test sets to assess whether the observed differences are statistically significant. To evaluate the robustness and consistency of the observed improvements, we ran this statistical analysis on both datasets (Dhaka and India-Nepal) separately across different distributions of data as shown in Table 8. The McNemar test reveals dataset dependency behavior. While gradient boosting significantly outperforms SVM on both datasets, no significant difference is observed with random forest and the voting classifier on the Dhaka dataset, whereas all comparisons are statistically significant on the India-Nepal dataset.

Table 8. McNemar test summary across datasets

Dataset	Algorithms	χ^2 statistic	Below threshold?	Summary	p-value
Dhaka	Gradient boosting vs SVC	3.890	YES	*	0.0486
Dhaka	Gradient boosting vs Random forest	0.356	NO	-	0.5510
Dhaka	Gradient boosting vs Voting classifier	0.138	NO	-	0.7103
India-Nepal	Gradient boosting vs SVC	4.085	YES	*	0.0433
India-Nepal	Gradient boosting vs Random forest	4.252	YES	*	0.0392
India-Nepal	Gradient boosting vs Voting classifier	10.588	YES	*	0.0011

Note: YES: significant ($p<0.05$); NO: not significant ($p\geq0.05$); the symbol (*) denotes statistical significance

5.4. Comparison and discussion

The results are compared with those of previous studies conducted on the same datasets. These comparisons are summarized in Table 9. Through this comparison, the effectiveness and robustness of the proposed approach can be clearly evaluated.

Results on the initial Dhaka dataset, on the first dataset collected from Dhaka, the proposed method based on feature fusion and grid search-optimized gradient boosting achieved an accuracy of 88.82%, which significantly outperforms the results reported by Mondal *et al.* [25], who obtained an accuracy of 70%. This represents an improvement of 18.82 percentage points, highlighting the strong discriminative capability of our classification-based framework. It is important to note that the method in [25] follows a regression strategy to directly estimate continuous $PM_{2.5}$ concentrations. To ensure a fair comparison, the predicted $PM_{2.5}$ values were converted into AQI categories using standard AQI thresholds (e.g., good, moderate, and unhealthy), allowing evaluation in a classification setting comparable to the approach.

Results on the second dataset from India-Nepal on the second dataset, which includes images from India-Nepal, our proposed method achieved an accuracy of 95.40%, outperforming several recent approaches reported in the literature. In particular, it exceeds the performance of Utomo *et al.* [27], who reported an accuracy of 89.38%, as well as Kushal and Al Mamun [41], whose multimodal CNN-based approach reached 92.02%, and Ozkok [42], who achieved 90.45% using transfer learning-based CNN models. These results demonstrate the superior generalization ability of the proposed method across different geographical regions and data characteristics.

Table 9. Comparison of AQI estimation accuracy between the proposed method and existing approaches

Study	Method	Dataset	Accuracy (%)
Mondal *et al.* [25]	DCNN	Dhaka	70.00
Proposed Method	Feature fusion + grid search (gradient boosting)	Dhaka	**88.82**
Utomo *et al.* [27]	Efficient CNN multimodal	India-Nepal	89.38
Kushal and Al Mamun [41]	CNN + sensor fusion	India-Nepal	92.02
Ozkok [42]	Transfer learning CNNs	India-Nepal	90.45
Proposed method	Feature fusion + grid search (gradient boosting)	India-Nepal	**95.40**

Overall, the performance gains can be attributed to the effective fusion of complementary visual quality descriptors. These gains are further supported by the integration of image-based meteorological and air quality indicators, and the use of robust machine learning classifiers optimized via grid search. Furthermore, the higher accuracy achieved on the India-Nepal dataset may be explained by its richer visual variability, which facilitates more discriminative feature learning and classification.

6. CONCLUSION

This paper presents a novel approach to estimate the AQI using visual quality analysis. Using the PPPC approach in conjunction with visual quality features and meteorological factors, we proposed a reliable model that can correctly identify the AQI. The outcomes from two different datasets show how robust and successful our method is, with excellent accuracy rates. The proposed approach provides a quick, accurate assessment based on photos and is therefore an acceptable alternative to traditional air quality monitoring techniques. Moreover, this approach has much to contribute in terms of accessibility and utility, especially in areas that are difficult to find or place monitoring stations. This study still exploring the potential for expanding the dataset and adding other features to enhance the quality of this method and its functionalities. We aim to create a Moroccan dataset that can help in reinforcing or improving the methodology. Developing a mobile application that takes an image of the environmental and tells the user if environment is contaminated or not will also be another goals for this work. In conclusion, this study provides innovative insight into the use of artificial intelligence and image technologies to assess the air quality, and subsequently opens the door for air quality management for, better health protection and environmental awareness.

ACKNOWLEDGMENTS

The authors would like to express sincere gratitude to the PROGRES-UCD program launched by Chouaib Doukkali University for supporting this research. This funding has played a crucial role in advancing our work and contributing to the scientific community.

FUNDING INFORMATION

This research was funded by Chouaib Doukkali University, Morocco, through the PROGRES-UCD program under grant number PROGRES 08/2024.

AUTHOR CONTRIBUTIONS STATEMENT

This journal uses the Contributor Roles Taxonomy (CRediT) to recognize individual author contributions, reduce authorship disputes, and facilitate collaboration.

Name of Author	C	M	So	Va	Fo	I	R	D	O	E	Vi	Su	P	Fu
Khadija Marzagui	✓	✓	✓	✓	✓	✓		✓	✓	✓	✓			
Yassine Benhlal		✓							✓	✓				
Abdelkaher Ait Abdelouahad	✓	✓		✓	✓	✓				✓	✓	✓		
Abdellatif Dahmouni	✓	✓		✓	✓	✓				✓	✓			
Ahmed Drissi El Maliani	✓	✓		✓	✓	✓				✓	✓	✓		
Hammadi Nait-Charif	✓	✓		✓	✓	✓				✓	✓			

C : **C**onceptualization
M : **M**ethodology
So : **So**ftware
Va : **Va**lidation
Fo : **Fo**rmal analysis
I : **I**nvestigation
R : **R**esources
D : **D**ata Curation
O : Writing - **O**riginal Draft
E : Writing - Review & **E**diting
Vi : **Vi**sualization
Su : **Su**pervision
P : **P**roject administration
Fu : **Fu**nding acquisition

CONFLICT OF INTEREST STATEMENT

Authors state no conflict of interest.

DATA AVAILABILITY

The data that support the findings of this study are available on request from the corresponding author, [KM]. The data, which include processed datasets and extracted feature values derived from third-party sources, are not publicly available due to certain restrictions.

REFERENCES

[1] K. L. Ebi and G. McGregor, "Climate change, tropospheric ozone and particulate matter, and health impacts," *Environmental Health Perspectives*, vol. 116, no. 11, pp. 1449–1455, Nov. 2008, doi: 10.1289/ehp.11463.

[2] E. G. Snyder *et al.*, "The changing paradigm of air pollution monitoring," *Environmental Science and Technology*, vol. 47, no. 20, pp. 11369–11377, Oct. 2013, doi: 10.1021/es4022602.

[3] Kanchan, A. K. Gorai, and P. Goyal, "A review on air quality indexing system," *Asian Journal of Atmospheric Environment*, vol. 9, no. 2, pp. 101–113, Jun. 2015, doi: 10.5572/ajae.2015.9.2.101.

[4] G. Zhang, "Progress of weather research and forecast (WRF) model and application in the United States," *Meteorological Monthly*, vol. 30, no. 12, pp. 27–31, 2004, doi: 10.7519/j.issn.1000-0526.2004.12.006.

[5] J. Chen, J. Lu, J. C. Avise, J. A. DaMassa, M. J. Kleeman, and A. P. Kaduwela, "Seasonal modeling of PM2.5 in California's San Joaquin Valley," *Atmospheric Environment*, vol. 92, pp. 182–190, Aug. 2014, doi: 10.1016/j.atmosenv.2014.04.030.

[6] P. E. Saide *et al.*, "Forecasting urban PM10 and PM2.5 pollution episodes in very stable nocturnal conditions and complex terrain using WRF-Chem CO tracer model," *Atmospheric Environment*, vol. 45, no. 16, pp. 2769–2780, 2011, doi: 10.1016/j.atmosenv.2011.02.001.

[7] K. Y. Chan and L. Jian, "Identification of significant factors for air pollution levels using a neural network based knowledge discovery system," *Neurocomputing*, vol. 99, pp. 564–569, 2013, doi: 10.1016/j.neucom.2012.06.003.

[8] Y. Tian *et al.*, "Advancing application of satellite remote sensing technologies for linking atmospheric and built environment to health," *Frontiers in Public Health*, vol. 11, Nov. 2023, doi: 10.3389/fpubh.2023.1270033.

[9] V. A. Nguyen, J. A. Starzyk, W. B. Goh, and D. Jachyra, "Neural network structure for spatio-temporal long-term memory," *IEEE Transactions on Neural Networks and Learning Systems*, vol. 23, no. 6, pp. 971–983, 2012, doi: 10.1109/TNNLS.2012.2191419.

[10] Y. Zheng, F. Liu, and H.-P. Hsieh, "U-Air," in *19th ACM SIGKDD international conference on Knowledge discovery and data mining*, New York, United States: ACM, Aug. 2013, pp. 1436–1444, doi: 10.1145/2487575.2488188.

[11] D. Hasenfratz, O. Saukh, C. Walser, C. Hueglin, M. Fierz, and L. Thiele, "Pushing the spatio-temporal resolution limit of urban air pollution maps," in *2014 IEEE International Conference on Pervasive Computing and Communications (PerCom)*, IEEE, Mar. 2014, pp. 69–77, doi: 10.1109/PerCom.2014.6813946.

[12] S. Devarakonda, P. Sevusu, H. Liu, R. Liu, L. Iftode, and B. Nath, "Real-time air quality monitoring through mobile sensing in metropolitan areas," in *2nd ACM SIGKDD International Workshop on Urban Computing*, New York, United States: ACM, Aug. 2013, pp. 1–8, doi: 10.1145/2505821.2505834.

[13] Y. Li, J. Huang, and J. Luo, "Using user generated online photos to estimate and monitor air pollution in major cities," in *7th International Conference on Internet Multimedia Computing and Service*, Aug. 2015, pp. 1–5, doi: 10.1145/2808492.2808564.

[14] C. Liu, F. Tsow, Y. Zou, and N. Tao, "Particle pollution estimation based on image analysis," *PLOS ONE*, vol. 11, no. 2, Feb. 2016, doi: 10.1371/journal.pone.0145955.

[15] Z. Zhang, H. Ma, H. Fu, L. Liu, and C. Zhang, "Outdoor air quality level inference via surveillance cameras," *Mobile Information Systems*, vol. 2016, pp. 1–10, 2016, doi: 10.1155/2016/9825820.

[16] Q. Chen, W. Chen, and G. Pan, "An improved picture-based prediction method of PM2.5 concentration," *IET Image Processing*, vol. 16, no. 11, pp. 2827–2833, Sep. 2022, doi: 10.1049/ipr2.12204.

[17] C. Zhang, J. Yan, C. Li, X. Rui, L. Liu, and R. Bie, "On estimating air pollution from photos using convolutional neural network," in *24th ACM international conference on Multimedia*, New York, United States: ACM, Oct. 2016, pp. 297–301, doi: 10.1145/2964284.2967230.
[18] A. Chakma, B. Vizena, T. Cao, J. Lin, and J. Zhang, "Image-based air quality analysis using deep convolutional neural network," in *2017 IEEE International Conference on Image Processing (ICIP)*, IEEE, Sep. 2017, pp. 3949–3952, doi: 10.1109/ICIP.2017.8297023.
[19] J. Ma, K. Li, Y. Han, P. Du, and J. Yang, "Image-based PM2.5 estimation and its application on depth estimation," in *2018 IEEE International Conference on Acoustics, Speech and Signal Processing (ICASSP)*, IEEE, Apr. 2018, pp. 1857–1861, doi: 10.1109/ICASSP.2018.8461776.
[20] M. Ahmed *et al.*, "AQE-Net: a deep learning model for estimating air quality of Karachi City from mobile images," *Remote Sensing*, vol. 14, no. 22, Nov. 2022, doi: 10.3390/rs14225732.
[21] Z. Xia, "A robust photo-based PM2.5_2.5 monitoring method by combining linear and non-linear learning," *IET Image Processing*, vol. 16, no. 4, pp. 1000–1007, Mar. 2022, doi: 10.1049/ipr2.12200.
[22] K. Gu, J. Qiao, and X. Li, "Highly efficient picture-based prediction of PM2.5 concentration," *IEEE Transactions on Industrial Electronics*, vol. 66, no. 4, pp. 3176–3184, Apr. 2019, doi: 10.1109/TIE.2018.2840515.
[23] N. Nilesh, I. Patwardhan, J. Narang, and S. Chaudhari, "IoT-based AQI estimation using image processing and learning methods," in *2022 IEEE 8th World Forum on Internet of Things (WF-IoT)*, IEEE, Oct. 2022, pp. 1–5. doi: 10.1109/WF-IoT54382.2022.10152272.
[24] K. Sun, L. Tang, S. Huang, and J. Qian, "A photo-based quality assessment model for the estimation of PM2.5 concentrations," *IET Image Processing*, vol. 16, no. 4, pp. 1008–1016, Mar. 2022, doi: 10.1049/ipr2.12201.
[25] J. J. Mondal *et al.*, "Uncovering local aggregated air quality index with smartphone captured images leveraging efficient deep convolutional neural network," *Scientific Reports*, vol. 14, no. 1, Jan. 2024, doi: 10.1038/s41598-023-51015-1.
[26] U.S. Environmental Protection Agency, *Technical assistance document for the reporting of daily air quality–the air quality index (AQI)*, North Carolina, United States: U.S. Environmental Protection Agency, 2018.
[27] S. Utomo *et al.*, "Eff-AQI: an efficient CNN-based model for air pollution estimation: a study case in India," in *Proceedings of the 2023 ACM Conference on Information Technology for Social Good*, New York, NY, USA: ACM, Sep. 2023, pp. 165–172, doi: 10.1145/3582515.3609531.
[28] MoEFCC, "National air quality index," *Central Pollution Control Board (CPCB)*, pp. 1–44, 2015.
[29] N. V. Chawla, K. W. Bowyer, L. O. Hall, and W. P. Kegelmeyer, "SMOTE: synthetic minority over-sampling technique," *Journal of Artificial Intelligence Research*, vol. 16, pp. 321–357, Jun. 2002, doi: 10.1613/jair.953.
[30] C. Avatavului and M. Prodan, "Evaluating image contrast: a comprehensive review and comparison of metrics," *Journal of Information Systems and Operations Management*, vol. 17, no. 1, 2023.
[31] C. E. Shannon, "A mathematical theory of communication," *Bell System Technical Journal*, vol. 27, no. 3, pp. 379–423, Jul. 1948, doi: 10.1002/j.1538-7305.1948.tb01338.x.
[32] K. He, J. Sun, and X. Tang, "Single image haze removal using dark channel prior," in *2009 IEEE Conference on Computer Vision and Pattern Recognition*, IEEE, Jun. 2009, pp. 1956–1963, doi: 10.1109/CVPR.2009.5206515.
[33] A. Mittal, A. K. Moorthy, and A. C. Bovik, "No-reference image quality assessment in the spatial domain," *IEEE Transactions on Image Processing*, vol. 21, no. 12, pp. 4695–4708, Dec. 2012, doi: 10.1109/TIP.2012.2214050.
[34] K. Gu, G. Zhai, W. Lin, and M. Liu, "The analysis of image contrast: from quality assessment to automatic enhancement," *IEEE Transactions on Cybernetics*, vol. 46, no. 1, pp. 284–297, Jan. 2016, doi: 10.1109/TCYB.2015.2401732.
[35] A. Mittal, R. Soundararajan, and A. C. Bovik, "Making a 'completely blind' image quality analyzer," *IEEE Signal Processing Letters*, vol. 20, no. 3, pp. 209–212, Mar. 2013, doi: 10.1109/LSP.2012.2227726.
[36] K. Gu, W. Lin, G. Zhai, X. Yang, W. Zhang, and C. W. Chen, "No-reference quality metric of contrast-distorted images based on information maximization," *IEEE Transactions on Cybernetics*, vol. 47, no. 12, pp. 4559–4565, Dec. 2017, doi: 10.1109/TCYB.2016.2575544.
[37] C. Cortes and V. Vapnik, "Support-vector networks," *Machine Learning*, vol. 20, no. 3, pp. 273–297, Sep. 1995, doi: 10.1007/BF00994018.
[38] L. Breiman, "Random forests," *Machine Learning*, vol. 45, no. 1, pp. 5–32, Oct. 2001, doi: 10.1023/A:1010933404324.
[39] J. H. Friedman, "Greedy function approximation: A gradient boosting machine.," *The Annals of Statistics*, vol. 29, no. 5, pp. 1189–1232, Oct. 2001, doi: 10.1214/aos/1013203451.
[40] T. G. Dietterich, "Ensemble methods in machine learning," in *Multiple Classifier Systems*, Berlin, Heidelberg: Springer, Jan. 2000, pp. 1–15, doi: 10.1007/3-540-45014-9_1.
[41] K. A. Kushal and A. Al Mamun, "AQFusionNet: multimodal deep learning for air quality index prediction with imagery and sensor data," 2025, *arXiv:2509.00353*.
[42] F. O. Ozkok, "Image-based air pollution classification using deep learning techniques," *Eurasia Proceedings of Science, Technology, Engineering and Mathematics*, vol. 35, pp. 302–313, 2025, doi: 10.55549/epstem.1806639.

BIOGRAPHIES OF AUTHORS



Khadija Marzagui obtained a master's degree in Business Intelligence and Big Data Analytics (BIBDA) in 2022 from the Faculty of Sciences, Chouaib Doukkali University, El Jadida, Morocco. She is currently a Ph.D. student in Artificial Intelligence and Image Processing at Chouaib Doukkali University. Her research interests include artificial intelligence, image quality assessment, and computer vision. In addition, she is a Ph.D. candidate at the Laboratory of Research in Optimization, Emerging Systems, Networks and Imaging (LAROSERI), Faculty of Sciences, Chouaib Doukkali University, El Jadida, Morocco. She can be contacted at email: khadijamarzagui@yahoo.com.



Yassine Benhlal received his master's degree in Business Intelligence and Big Data Analytics (BIBDA) in 2024 from the Faculty of Sciences, Chouaib Doukkali University, El Jadida, Morocco. He is currently a Ph.D. student at Chouaib Doukkali University. His research interests include artificial intelligence, machine learning, deep learning, and image processing. In addition, he is a Ph.D. candidate at the Optimization Research Emerging Systems, Networks, and Imaging Laboratory (LAROSERI), Faculty of Sciences, Chouaib Doukkali University, El Jadida, Morocco. He can be contacted at email: benhlal.y@ucd.ac.ma.



Abdelkaher Ait Abdelouahad is a full professor at Chouaib Doukkali University (El Jadida, Morocco). He holds a bachelor's degree in Computer Science and Mathematics (2006) and a master's degree in Computer Science and Telecommunications (2008). He earned his Ph.D. in 2013, with a dissertation focused on computer vision and, more specifically, image quality assessment. From 2013 to 2019, he served as an assistant professor at Ibn Zohr University. He then joined Chouaib Doukkali University as an associate professor until 2024, and currently holds the position of full professor. He leads the research team "Artificial Intelligence and Multimedia" within the LAROSERI Laboratory and coordinates the master's program in Business Intelligence and Big Data Analytics. His research interests include artificial intelligence, computer vision, and data analytics. He can be contacted at email: a.abdelkaher@gmail.com.



Abdellatif Dahmouni received his Ph.D. from the Faculty of Sciences (Fes, Morocco) in 2019. He is currently a qualified professor in Computer Science at the Higher School of Technology of Moulay Ismail University (Meknes, Morocco). From 2020 to 2025, he served as an assistant professor of Computer Science at the Faculty of Sciences of Chouaib Doukkali University (El Jadida, Morocco). His research, conducted within the IMACS Laboratory, focuses on artificial intelligence and learning theory, graph theory and complex networks, data visualization and information retrieval, as well as pattern recognition and computer vision. He can be contacted at email: a.dahmouni@umi.ac.ma.



Ahmed Drissi El Maliani is a full professor at the Faculty of Sciences of Rabat, Mohammed V University, Morocco where he is affiliated with the LRIT Laboratory. He received a Ph.D. degree in engineering sciences from the same University. This latter concerned stochastic modeling of natural images with applications in content-based texture retrieval and classification. He has co-authored many journal articles, conference publications, and book chapters. His current research mainly focuses on information geometry, machine learning, and medical image analysis, especially in the field of neuroscience. He is a member of numerous national and international conference committees and serves as a reviewer of well-known journals in the field. He is also a member and vice-president of the Moroccan Mobile Computing and Intelligent Embedded-Systems Society (Mobitic, http://www.mobitic.org/). He can be contacted at email: a.elmaliani@um5r.ac.ma.



Hammadi Nait-Charif is an associate professor at Bournemouth University, United Kingdom, specializing in artificial intelligence, computer vision, and human-computer interaction. He holds a Ph.D. in Information and Computer Sciences from Chiba University, Japan and an engineering degree in Electronics from Ecole Hassania in Casablanca, Morocco. His career includes various roles in academia and research. He was a teaching assistant at Chiba University, Japan. He was also an assistant professor and head of the Electrical and Department of Electronic Engineering at Mohamed I University in Morocco. In 1999, he was a fulbright visiting scholar at Michigan State University, United States, and in 2001 he joined Dundee University, Scotland as a postdoc then as a teaching fellow. His research focuses on intelligent systems, machine learning, computer vision, image processing, and virtual/augmented reality. He has published extensively in peer-reviewed journals and conferences and is actively involved in interdisciplinary projects combining technology with healthcare. He can be contacted at email: hncharif@bournemouth.ac.uk.